Bioorganic & Medicinal Chemistry 18 (2010) 1312–1320

Contents lists available at ScienceDirect

Bioorganic & Medicinal Chemistry

journal homepage: www.elsevier.com/locate/bmc

Preparation and biodistribution of [^{18}F]FP2OP as myocardial perfusion imaging agent for positron emission tomography

Tiantian Mou [a], Huihui Jing [a], Wenjiang Yang [a], Wei Fang [b], Cheng Peng [c], Feng Guo [b], Xianzhong Zhang [a,*], Yan Pang [a], Yunchuan Ma [c]

[a] Key Laboratory of Radiopharmaceuticals, Ministry of Education, College of Chemistry, Beijing Normal University, 19 Xinjiekou Outer St., Beijing 100875, China
[b] Department of Nuclear Medicine, Cardiovascular Institute and Fu Wai Hospital, Chinese Academy of Medical Sciences, Beijing 100037, China
[c] PET Center of Xuan Wu Hospital, Capital Medical University, Beijing 100053, China

ARTICLE INFO

Article history:
Received 15 October 2009
Revised 6 December 2009
Accepted 8 December 2009
Available online 26 December 2009

Keywords:
Positron emission tomography
Myocardial perfusion imaging
[^{18}F]FP2OP
Mitochondria complex I

ABSTRACT

Myocardial extractions of pyridaben, a mitochondrial complex I (MC-I) inhibitor, is well correlated with blood flow. Based on the synthesis and characterization of pyridaben analogue 2-*tert*-butyl-5-[2-(2-[^{18}F]fluroethoxy)ethoxy]benzyloxy]-4-chloro-2*H*-pyridazin-3-one ([^{18}F]FP2OP), this study assessed its potential to be developed as myocardial perfusion imaging (MPI) agent.

Methods: The tosylate labeling precursor 2-(2-(4-(*tert*-butyl-5-chloro-6-oxo-1,6-dihydro-pyridazin-4-yloxymethyl)benzyloxy)ethoxy)ethyl ester (OTs-P2OP) and the nonradioactive 2-*tert*-butyl-5-[2-(2-[^{19}F]fluroethoxy)ethoxy]benzyloxy]-4-chloro-2*H*-pyridazin-3-one ([^{19}F]FP2OP) were synthesized and characterized by IR, ^{1}H NMR, ^{13}C NMR and MS analysis. By substituting tosyl of precursor OTs-P2OP with ^{18}F, the radiolabeled complex [^{18}F]FP2OP was prepared and further evaluated for its in vitro physico-chemical properties, in vivo biodistribution, the metabolic stability in mice, ex vivo autoradiography and cardiac PET/CT imaging.

Results: Starting with [^{18}F]F^- Kryptofix 2.2.2./K_2CO_3 solution, the total reaction time for [^{18}F]FP2OP was about 100 min, with final high-performance liquid chromatography purification included. Typical decay-corrected radiochemical yield stayed at 41 ± 5.3%, the radiochemical purity, 98% or more. Biodistribution in mice showed that the heart uptake of [^{18}F]FP2OP was 41.90 ± 4.52%ID/g at 2 min post-injection time, when the ratio of heart/liver, heart/lung and heart/blood reached 6.83, 9.49 and 35.74, respectively. Lipophilic molecule was further produced by metabolized [^{18}F]FP2OP in blood and urine at 30 min. Ex vivo autoradiography demonstrates that [^{18}F]FP2OP may have high affinity with MC-I and that can be blocked by [^{19}F]FP2OP or rotenone (a known MC-I inhibitor). Cardiac PET images were obtained in a Chinese mini-swine at 5, 15, 30 and 60 min post-injection time with high quality.

Conclusion: [^{18}F]FP2OP was synthesized with high radiochemical yield. The promising biological properties of [^{18}F]FP2OP suggest high potential as MPI agent for positron emission tomography in the future.

1. Introduction

Coronary artery disease (CAD) is the leading cause of death in developed countries and is a serious health problem worldwide. Myocardial perfusion imaging (MPI), an aid in clinical diagnosis, plays an important role in noninvasive measurement of CAD. Currently, MPI is performed with six agents in clinic use: [^{201}Tl]TlCl, ^{99m}Tc-sestamibi, ^{99m}Tc-tetrofosmin, [^{82}Rb]RbCl, [^{13}N]NH_3, and [^{15}O]H_2O.[1] The first three of these tracers being single-photon-emitting agents, which serve as the mainstay of myocardial perfusion imaging (MPI) tests.[2] However, positron emission tomography (PET) imaging provides certain advantages versus single-photon emission computed tomography (SPECT), including higher spatial resolution, improved attenuation correction, and the capability to perform quantitative measurements at the peak of stress. Given this situation, there is a well-recognized need for the development of new perfusion tracers with more ideal properties for PET imaging. Cardiac PET, accordingly, has an opportunity to become the standard for evaluation of myocardial perfusion in coming years.[3]

Mitochondria, known as the powerhouse of the cell, are abundant in tissues with large energy requirements, such as the heart, where they take up 20–30% of the myocardial intracellular volume.[4] Therefore, a couple of MPI agents, such as ^{18}FTPP, [^{18}F]FBnTP, BMS-747158–02, take mitochondria as their target.[2,5,6] Four electron transport complexes are located in the inner mitochondrial membrane, of which MC-I is the first enzyme. Recent studies showed that ^{18}F- or ^{125}I-labeled MC-I inhibitors was highly

* Corresponding author. Tel.: +86 10 58802038; fax: +86 10 62208126.
E-mail addresses: zhangxzh@gmail.com, zhangxzh@bnu.edu.cn (X. Zhang).

0968-0896/$ - see front matter © 2009 Elsevier Ltd. All rights reserved.
doi:10.1016/j.bmc.2009.12.022

correlated with flow.[7–9] Accordingly, we designed a new [^{18}F]-labeled tracer based on pyridaben, one of MC-I inhibitors, for myocardial perfusion imaging.

Here we report the synthesis and characterization of pyridaben analogue 2-*tert*-butyl-5-[2-(2-[^{18}F]fluroethoxy)ethoxy]benzyloxy]-4-chloro-2*H*-pyridazin-3-one ([^{18}F]FP2OP) as a potential myocardial perfusion imaging (MPI) agent.

2. Materials and methods

2.1. Materials

[^{18}F]F^- was obtained from PET Center of Xuanwu Hospital (Beijing, China). No-carrier-added [^{18}F]F^- was trapped on a QMA cartridges and eluted with 0.3 mL K_2CO_3 solution (10 mg/mL in H_2O) combined with 1 mL Kryptofix2.2.2. solution (Sigma–Aldrich) (13 mg/mL in acetonitrile).[10,11] Instant lyophilized Kit for ^{99m}Tc-MIBI (MIBI = 2-methoxyisobutylisonitrile) preparation was donated by Beijing SHIHONG Pharmaceutical Co., Ltd (Beijing, China). ^{99m}Tc-MIBI injection was prepared under Kit instruction. Rotenone with 95% purity was purchased from Sigma–Aldrich. Other reagents and solvents were purchased from commercial suppliers and were used without further purification. Paper electrophoresis experiments were carried out using 0.025 mol/L phosphate buffer (pH 7.4) and Xinhua 1# filter paper at 150 V for 180 min. Reversed-phase high-pressure liquid chromatography (RP-HPLC) was performed on an Alltech system with Alltech HPLC pump Model 626, LINEAR UVIS-201, and BIOSCAN flow-counter. The C-18 reverse-phase Semi-Preparative HPLC column (10 × 250 mm, 5 μm particle size, Venusil MP-C18, Agela Technologies Inc., USA) was eluted at a flow rate of 5 mL/min. Labgen 7 homogenizer was purchased from Cole-Parmer Instrument (USA).

^{1}H NMR spectra were recorded on a Bruker (400 MHz) spectrometer, while ^{13}C NMR spectra were recorded on a Bruker (100 MHz) spectrometer. Chemical shifts are reported in δ (ppm) values. Infrared spectra were measured on a Nicolet 360 Avatar instrument using a potassium bromide (KBr) disk, scanning from 400 to 4000 cm^{-1}. Mass spectra were recorded using a Brucker Apex IV FTM instrument.

2.2. Preparation of 2,3-dichloro-4-oxo-2-butenoicacid (DCA)

The synthesis route of DCA, shown in Figure 1, is a slight modification of the procedure described by Feng et al.[12]

MnO_2 (80 g, 0.9 mol) was added to concentrated hydrochloric acid (480 mL, 5.8 mol) in portions with ice-bath cooling. Furfural

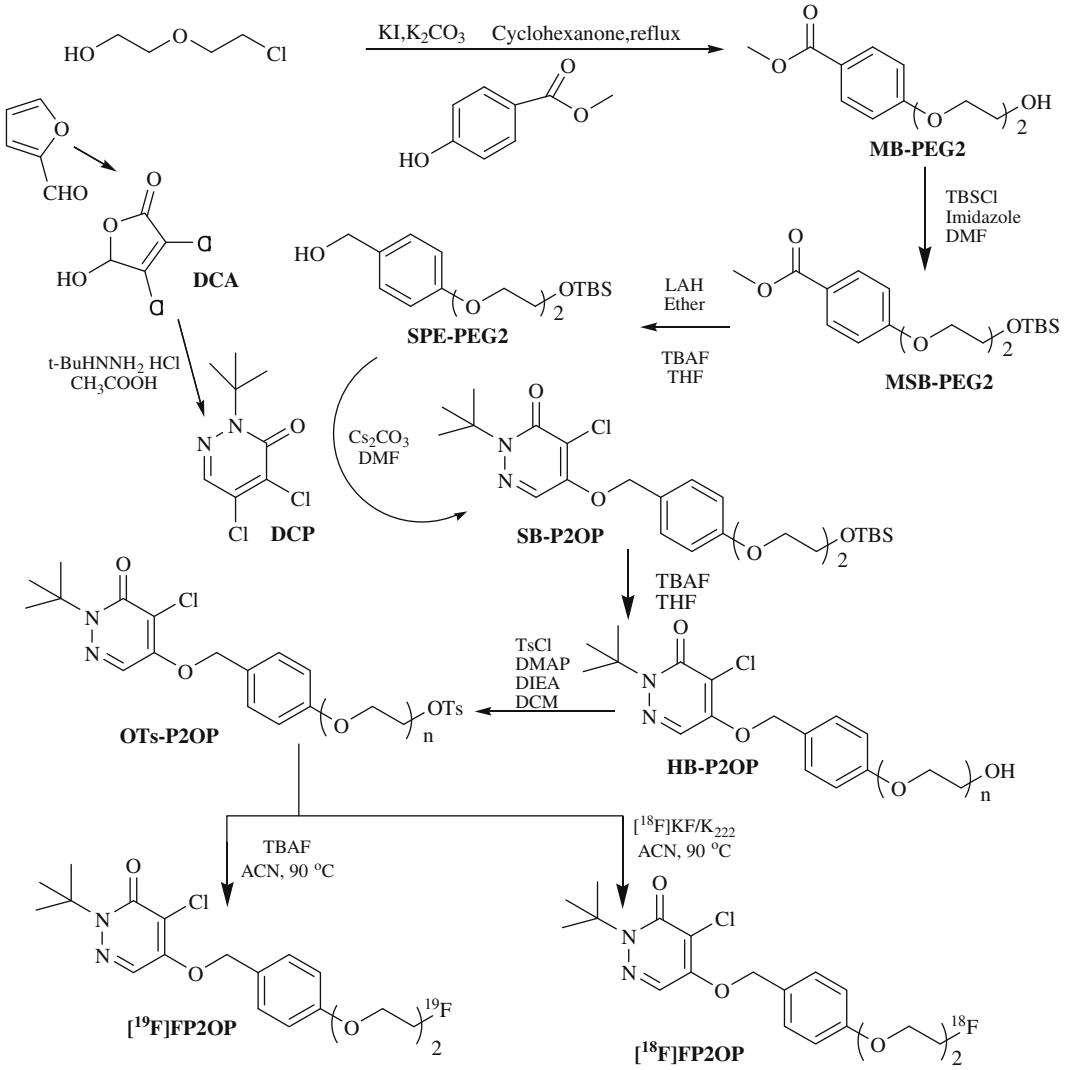

Figure 1. The synthesis route of OTs-P2OP, nonradioactive [^{19}F]FP2OP and [^{18}F]FP2OP .

(24 g, 0.25 mol) slowly dropped into the reaction flask at 0–10 °C, stirring for 30 min, then heated to 60 °C. MnO_2 (42 g, 0.5 mol) was added in portion at 60–80 °C, heated to 100 °C, stirred until the solution turned to orange, then cooled to room temperature. After filtration, filter residue was dissolved in ether (40 mL), and filtered again. Filtrate was concentrated in vacuo. The residue was recrystalled from water (40 mL) to get DCA as a white crystal (yield: 25 g, 59%). ^{1}H NMR, ^{13}C NMR and IR for DCA: ^{1}H NMR (400 MHz, $CDCl_3$) δ: 6.085 (s, 1H, HO–C–*H*); ^{13}C NMR (100 MHz, $CDCl_3$) δ: 98.56, 123.87, 151.25, 165.15; IR (KBr, cm^{-1}) ν: 3407 (O–H), 1770 (C=O), 1638 (C=C).

2.3. Preparation of 2-*tert*-butyl-4.5-dichloro-2*H*-pyridazin-3-one (DCP)

The synthesis route of DCP is shown in Figure 1. DCA (15 g, 0.09 mol) and Na_2CO_3 (4.5 g, 0.04 mol) were added to 150 mL water in an ice bath, stirred until the reaction mixture became clarifying. *tert*-Butyl hydrazine hydrochloride (11 g, 0.09 mol) was added into the reaction flask and stirred for 2.5 h, then filtered. The filter residue was washed by cool water, and transferred into a 100 mL flask. Benzene (50 mL) and acetic acid (7 g) were added to the flask above, and then the mixture was heated to 35–45 °C and stirred for 4 h. The mixture was washed by 20 mL water and then the organic phase was separated and washed by 20 mL NaOH solution (1.25 mol/L), 20 mL HCl solution (3 mol/L) and 20 mL water successively. The organic layer was dried with $MgSO_4$, filtered, and most of solvent removed under reduced pressure. The residue was crystalled to get DCP as a buff crystal (yield: 7.6 g, 38%). ^{1}H NMR and IR for DCP: ^{1}H NMR (400 MHz, $CDCl_3$) δ: 1.648 (s, 9H, N(CH_3)$_3$), 7.729 (s, 1H, N=C–*H*); IR (KBr, cm^{-1}) ν: 3461 (O–H), 1658 (C=O).

2.4. Preparation of methyl 4-[2-(2-hydroxyethoxy)ethoxy]-benzoate (MB-PEG2)

The synthesis route of MB-PEG2, shown in Figure 1, is a slight modification of the procedure described by Bender et al.[13]

Cyclohexanone (20 mL) was added to a mixture of methyl-4-hydroxybenzoate (1 g, 6.57 mmol), KI (0.55 g, 3.29 mmol), and K_2CO_3 (1.81 g, 13.1 mmol) with stirring under nitrogen. 2-(2-Chloroethoxy)ethanol (1.8 mL, 17.0 mmol) was added into the reaction flask, and refluxed with stirring for 1 d under nitrogen. The suspension was cooled to room temperature and filtered to remove the solids. The yellow-orange filtrate was concentrated in vacuo. After that, CH_2Cl_2 (15 mL) was added to the residue, filtered, and the filtrate was concentrated in vacuo again. The residue was chromatographed over a column of silica gel and eluted with ether to give the MB-PEG2 as buff oil (yield: 1.04 g, 66%). ^{1}H NMR and IR for MB-PEG2: ^{1}H NMR (400 MHz, $CDCl_3$) δ: 2.072 (s, 1H, O*H*), 3.677 (t, 2H, CH_2CH_2OH), 3.769 (t, 2H, CH_2CH_2OH), 3.883 (s, 3H, OCH_3), 3.886 (t, 2H, phenyl-O-CH_2CH_2), 4.191 (t, 2H, phenyl-O-CH_2), 6.934 (d, 2H, O-*phenyl*), 7.986 (d, 2H, CO-*phenyl*); IR (KBr, cm^{-1}) ν: 3461 (O–H), 1715 (C=O), 1102 (C–O–C).

2.5. Preparation of methyl 4-[2-(2-(*tert*-butyldimethylsiloxy)-ethoxy)ethoxy]benzoate (MSB-PEG2)

The synthesis route of MSB-PEG2, shown in Figure 1, is a slight modification of the procedure described by Caesbier et al.[14]

Anhydrous DMF (10 mL) was added into the mixture of imidazole (0.50 g, 7.2 mmol), MB-PEG2 (1.04 g, 4.3 mmol) and *tert*-butyldimethylsilyl chloride (1.08 g, 7.4 mmol). After stirring in an oil bath for 4 h at 80 °C, the reaction mixture was diluted with ethyl acetate (20 mL) and extracted five times with saturated NaCl solution (20 mL for each extraction), then extracted two times with saturated $NaHCO_3$ (20 mL for each extraction). The organic phase was dried with $MgSO_4$, filtered, and concentrated under reduced pressure to give MSB-PEG2 as buff oil (yield: 1.07 g, 70%). ^{1}H NMR and IR for MSB-PEG2: ^{1}H NMR (400 MHz, $CDCl_3$) δ: 0.000 (s, 6H, OSi(CH_3)$_2$), 0.824 (s, 9H, SiC(CH_3)$_3$), 3.567 (t, 2H, CH_2CH_2O-Si), 3.726 (t, 2H, CH_2CH_2OSi), 3.813 (s, 3H, OCH_3), 3.815 (t, 2H, phenyl-O-CH_2CH_2), 4.099 (t, 2H, phenyl-O-CH_2), 6.862 (d, 2H, O-*phenyl*), 7.911 (d, 2H, CO-*phenyl*); IR (KBr, cm^{-1}) ν: 1723 (C=O), 1250 (=C–O–C), 1087 (C–O–C).

2.6. Preparation of 4-[2-(2-(*tert*-butyldimethylsiloxy)ethoxy)-ethoxy]phenylethanol (SPE-PEG2)

The synthesis route of SPE-PEG2 is based on the procedure described by Caesbier et al.[14] with a slight modification (Fig. 1).

The solution of MSB-PEG2 (1.07 g, 3 mmol in 15 mL ether) was dropped slowly into the mixture of anhydrous ether (10 mL) and $LiAlH_4$ (0.28 g, 7.2 mmol), stirring in the ice bath for 2 h, then stirring for another 2 h at room temperature. The water was dropped slowly into the flask until no gas produced, and then the pH was adjusted to 6. After filtered, filtrate was dried with $MgSO_4$, filtered, and concentrated to give SPE-PEG2 as buff oil (yield: 0.93 g, 95%). ^{1}H NMR for SPE-PEG2: ^{1}H NMR (400 MHz, $CDCl_3$) δ: 0.000 (s, 6H, OSi(CH_3)$_2$), 0.815 (s, 9H, SiC(CH_3)$_3$), 3.580 (t, 2H, CH_2CH_2OSi), 3.672 (t, 2H, CH_2CH_2OSi), 3.775 (t, 2H, phenyl-O-CH_2CH_2), 4.046 (t, 2H, phenyl-O-CH_2CH_2), 4.466 (s, 2H, CH_2–O–C=C–Cl), 6.807 (d, 2H, O-*phenyl*), 7.211 (d, 2H, CO-*phenyl*).

2.7. Preparation of 2-*tert*-butyl-5-[2-(2-(*tert*-butyldimethylsiloxy)-ethoxy)ethoxy]benzyloxy-4-chloro-2*H*-pyridazin-3-one (SB-P2OP)

The synthesis route of SB-P2OP, shown in Figure 1, is a slight modification of the procedure described by Caesbier et al.[14]

Anhydrous DMF (10 mL) was added to the mixture of SPE-PEG2 (0.38 g, 1.2 mmol), DCP (0.93 g, 4.2 mmol) and Cs_2CO_3 (1.37 g, 4.2 mmol), and stirred for 12 h at 68 °C in an oil bath. After cooled to temperature, the reaction solution was diluted with ethyl acetate (20 mL), and washed five times by saturated NaCl solution (20 mL for each time). The organic phase was dried with $MgSO_4$, filtered, and concentrated under reduced pressure. The residue was chromatographed over a column of silica gel and eluted with the mixture of hexane and ethyl acetate 3:1 (v/v). After removal of the solvents under vacuum, SB-P2OP was obtained as buff oil (yield: 0.55 g, 90%). ^{1}H NMR and IR for SB-P2OP: ^{1}H NMR (400 MHz, $CDCl_3$) δ: 0.000 (s, 6H, OSi(CH_3)$_2$), 0.824 (s, 9H, SiC(CH_3)$_3$), 1.558 (s, 9H, N(CH_3)$_3$), 3.566 (t, 2H, CH_2CH_2OSi), 3.727 (t, 2H, CH_2CH_2OSi), 3.802 (t, 2H, phenyl-O-CH_2CH_2), 4.057 (t, 2H, phenyl-OCH_2CH_2), 5.177 (s, 2H, CH_2–O–C=C–Cl), 6.876 (d, 2H, O-*phenyl*), 7.255 (d, 2H, CO-*phenyl*), 7.663 (s, 1H, N=C-*H*); IR (CH_2Cl_2, cm^{-1}) ν: 1649 (C=O), 1250 (=C–O–C), 1132 (C–O–C).

2.8. Preparation of 2-*tert*-butyl-5-[2-(2-hydroethoxy)ethoxy]-benzyloxy]-4-chloro-2*H*-pyridazin-3-one (HB-P2OP)

The synthesis route of HB-P2OP, shown in Figure 1, is a slight modification of the procedure described by Caesbier et al.[14]

Anhydrous tetrahydrofuran (3 mL) was added to the mixture of SB-P2OP (552 mg, 1.1 mmol) and *tert*-butylammonium fluoride (3 mmol in 3 mL tetrahydrofuran). After stirring for 2 h, the reaction solution was diluted with ethyl acetate (20 mL), and extracted two times with saturated NaCl solution (20 mL for each extraction). The organic layer was separated and dried with $MgSO_4$, filtered, and concentrated under reduced pressure. The residue was chromatographed over a column of silica gel and eluted with the mixture of CH_2Cl_2 and CH_3OH 7:1 (v/v). After re-

moval of the solvents under vacuum, HB-P2OP was obtained as yellow oil (yield: 361 mg, 83%). ^{1}H NMR and IR for HB-P2OP: ^{1}H NMR (400 MHz, $CDCl_3$) δ: 1.532 (s, 9H, N(CH_3)$_3$), 3.586 (t, 2H, CH_2CH_2OH), 3.678 (t, 2H, CH_2CH_2OH), 3.785 (t, 2H, phenyl-O-CH_2CH_2), 4.059 (t, 2H, phenyl-OCH_2CH_2), 5.153 (s, 2H, CH_2–O–C=C–Cl), 6.857 (d, 2H, O-*phenyl*), 7.240 (d, 2H, CO-*phenyl*), 7.636 (s, 1H, N=C–*H*); IR (CH_2Cl_2, cm^{-1}) *v*: 3239 (O–H), 1643 (C=O), 1251 (=C–O–C), 1137 (C–O–C).

2.9. Preparation of toluene-4-sulfonic acid 2-*tert*-butyl-4-chloro-5-[2-(2-(*tert*-butyldimethylsilanyloxy)ethoxy)ethoxy]-benzyloxy-2*H*-pyridazin-3-one (OTs-P2OP)

The synthesis route of OTs-P2OP, shown in Figure 1, is a slight modification of the procedure described by Caesbier et al.[14]

Anhydrous CH_2Cl_2 (3 mL) was added to the mixture of HB-P2OP (361 mg, 0.91 mmol), TsCl (252 mg, 1.32 mmol), 4-dimethylaminopyridine (167 mg, 1.37 mmol) and *N*,*N*-diisopropylethylamine (175 mg, 1.35 mmol). After stirring for 2 h, the reaction mixture was diluted with ethyl acetate (20 mL), and filtered. The filtrate was washed with 0.1 mol/L HCl (20 mL) and saturated NaCl solution (20 mL). The organic phase was separated and dried with $MgSO_4$, filtered, and concentrated under reduced pressure. The residue was chromatographed over a column of silica gel and eluted with the mixture of CH_2Cl_2 and CH_3OH 100:1 (v/v). After removal of the solvents under vacuum, OTs-P2OP was obtained as yellow solid (yield: 260 mg, 51%). ^{1}H NMR, ESI-MS and IR for OTs-P2OP: ^{1}H NMR (400 MHz, $CDCl_3$) δ: 1.558 (s, 9H, N(CH_3)$_3$), 2.341 (s, 3H, phenyl-CH_3), 3.695 (t, 2H, CH_2CH_2OS), 3.729 (t, 2H, CH_2CH_2OS), 3.990 (t, 2H, phenyl-O-CH_2CH_2), 4.122 (t, 2H, phenyl-OCH_2CH_2), 5.180 (s, 2H, CH_2–O–C=C–Cl), 6.850 (d, 2H, O-*phenyl*), 7.235 (d, 2H, CO-*phenyl*), 7.265 (d, 2H, *phenyl*-CH_3), 7.666 (s, 1H, N=C–*H*), 7.723 (d, 2H, *phenyl*-SO_3); ESI-MS calculated for $C_{26}H_{31}ClN_2O_7S$: 550.1. Found 551.2 [M+1]$^+$; IR (CH_2Cl_2, cm^{-1}) *v*: 1652 (C=O), 1249 (=C–O–C), 1092 (C–O–C).

2.10. Preparation of nonradioactive 2-*tert*-butyl-5-[2-(2-fluroethoxy)ethoxy]benzyloxy-4-chloro-2*H*-pyridazin-3-one ([^{19}F]FP2OP)

The synthesis route of [^{19}F]FP2OP, shown in Figure 1, is a slight modification of the procedure described by Caesbier et al.[14]

The solution of *tert*-butylammonium fluoride (1 mmol in 1 mL tetrahydrofuran) was added to a 25 mL flask. After evaporation in a stream of nitrogen at 110 °C, the labeling precursor OTs-P2OP (260 mg, 0.47 mmol in 3 mL anhydrous CH_3CN) was added to the above evaporation residue, and refluxed for 40 min at 90 °C. Then the reaction solution was evaporated again and the residue was diluted with CH_2Cl_2 (15 mL), and washed with saturated NaCl solution (20 mL). After concentrated under reduced pressure, the residue was chromatographed over a column of silica gel and eluted with the mixture of CH_2Cl_2 and CH_3OH 100:1 (v/v). [^{19}F]FP2OP was obtained as brown solid (yield: 150 mg, 80%). ^{1}H NMR, ^{13}C NMR, ^{19}F NMR, ESI-MS and IR for [^{19}F]FP2OP: ^{1}H NMR (400 MHz, $CDCl_3$) δ: 1.554 (s, 9H, N(CH_3)$_3$), 3.744 (dt, 2H, CH_2CH_2OF), 3.820 (t, 2H, phenyl-O-CH_2CH_2), 4.081 (t, 2H, phenyl-OCH_2CH_2), 4.514 (dt, 2H, CH_2CH_2OF), 5.167 (s, 2H, CH_2–O–C=C-Cl), 6.873 (d, 2H, O-*phenyl*), 7.252 (d, 2H, CO-*phenyl*), 7.656 (s, 1H, N=C–*H*); ^{13}C NMR (100 MHz; $CDCl_3$) δ: 26.87, 65.33, 66.57, 68.86, 69.60 (d, J = 9 Hz), 70.80, 82.11 (d, J = 84 Hz), 114.06, 117.32, 124.35, 126.20, 127.94, 152.78, 158.07, 158.17; ^{19}F NMR δ: −222.86; ESI-MS calculated for $C_{19}H_{24}ClFN_2O4$: 398.1. Found 399.1 [M+1]$^+$; IR (CH_2Cl_2, cm^{-1}) *v*: 1641 (C=O), 1242 (=C–O–C), 1091 (C–O–C).

2.11. Preparation of 2-*tert*-butyl-5-[2-(2-[^{18}F]fluroethoxy)-ethoxy]benzyloxy-4-chloro-2*H*-pyridazin-3-one ([^{18}F]FP2OP)

[^{18}F]F$^-$ was eluted from the QMA cartridges with the solution of K_2CO_3 (3 mg in 0.3 mL H_2O) combined with the solution of Kryptofix2.2.2 (13 mg in 1 mL acetonitrile). The liquid evaporated under a stream of nitrogen at 110 °C. The labeling precursor OTs-P2OP (2 mg, 3.6 μmol) was dissolved in anhydrous acetonitrile (1 mL) and added to the above evaporation residue. After stirring for 30 min at 90 °C, it was cooled to room temperature and the solution was diluted with 9 mL water, and trapped on a C-18 Sep-Pak cartridge. [^{18}F]FP2OP was eluted to a 10 mL vial with 3 mL CH_2Cl_2. After the solvent CH_2Cl_2 was removed under a stream of nitrogen at 60 °C, the residue was dissolved in 0.5 mL acetonitrile and injected onto a semi-HPLC column for purification. The column was eluted with water (solvent A) and acetonitrile (solvent B) at a flow rate of 5.0 mL/min. Gradient: 0–5 min: 95% A, 5.01–8 min: 95–60% A, 8.01–16 min: 60–35% A, 16.01–30 min: 0% A. The desired product was collected from HPLC and the solvent evaporated using a rotary evaporator. The product was redissolved in 5% ethanol solution, and filtered through a 0.22 μm Millipore filter.

Specific activity was calculated by measuring the radioactivity of the product fraction in the dose calibrator and dividing the value by the mass of the product as determined by the area under the UV curve measured at 254 nm. Chemical and radiochemical purity was checked by re-injection of the product onto a radio-HPLC, the radioactive fraction was collected and radioactivity was measured.

2.12. Octanol/water partition coefficient[15,16]

The octanol/water partition coefficient of [^{18}F]FP2OP was measured following 1 min vigorous vortex mixing of 500 μL octanol and 500 μL phosphate buffer (0.025 mol/L, pH 7.4), with approximately 74 kBq of radiotracer in a microcentrifuge tube. The tube was centrifuged at 6000 rpm for 5 min and the counts in 100 μL aliquots of both organic and aqueous layers were determined using a 1470 Wizard™ Automatic Gamma Counter (Perkin-Elmer). The measurement was repeated three times. Care was taken to avoid cross contamination between the phases. The partition coefficient (P) was calculated using the following equation: P = (cpm in the octanol phase − background cpm)/(cpm in the aqueous phase − background cpm). The partition coefficient value was expressed as log P.

2.13. Stability study

Purified [^{18}F]FP2OP solution (~3.7 MBq, in 100 μL water) was incubated at room temperature for 1 h. The radiochemical purity (RCP) was assayed by HPLC at 1 h after preparation. In order to test the stability of [^{18}F]FP2OP in organic solvent, the purified [^{18}F]FP2OP (~3.7 MBq) was dissolved in 100 μL of 80% ethanol solution and incubated at room temperature for 4 h. The radiochemical purity was assayed by HPLC at 4 h after preparation.

The stability in mouse plasma was determined by incubating ~3.7 MBq purified [^{18}F]FP2OP in the solution of 0.5 mL murine plasma at 37 °C for 1 h. Plasma proteins were precipitated by adding 100 μL acetonitrile and removed by centrifugation at 6000 rpm for 5 min at room temperature. The radiochemical purity was analyzed by HPLC.

2.14. Paper electrophoresis[15]

Paper electrophoresis experiments were performed on Xinhua filter papers (10 cm × 1 cm) which were pre-treated with phosphate buffer (0.025 mol/L, pH 7.4). The analyses were carried out using phosphate buffer (0.025 mol/L, pH 7.4) at 150 V for

180 min. The developed paper strips were left to dry and the distribution of radioactivity on the strip was determined using a 1470 Wizard™ Automatic Gamma Counter.

2.15. Biodistribution study

All the animal studies were carried out in compliance with relevant national laws relating to the conduct of animal experimentation.

The in vivo biodistribution study of [^{18}F]FP2OP was carried out in normal Kunming mice (18–20 g) obtained from the Animal Center of Peking University. About 185 kBq [^{18}F]FP2OP in 0.1 mL 5% ethanol solution was injected through the tail vein (5 animals per group). The mice were sacrificed at 2, 15, 30 and 60 min post-injection and the tissues and organs of interest were collected, wet weighed and counted in a 1470 Wizard™ Automatic Gamma Counter. The percentage of injected dose per gram (% ID/g) for each sample was calculated by comparing its activity with that of an appropriate aliquot of the injection solution, the values expressed as mean ± 1 standard deviation (SD).

In order to compare this new PET tracer ([^{18}F]FP2OP) with the traditional SPECT myocardial perfusion imaging agent: ^{99m}Tc-MIBI, the biodistribution study of ^{99m}Tc-MIBI was performed at the same condition described as above.

2.16. Metabolic stability[17,10,18]

Normal Kunming mice (18–20 g) were intravenously injected with 3.7 MBq of the [^{18}F]FP2OP injection solution. The animals were sacrificed and dissected at 2, 30 and 60 min after tracer injection. Blood was sampled after decapitation, and immediately centrifuged at 6000 rpm for 5 min. Urine was sampled from the urinary bladder, and directly diluted with 1 mL of phosphate buffered saline (PBS) (0.025 mol/L, pH 7.4) and then passed through a Sep-Pak C18 cartridge. The cartridges were washed with 0.5 mL water and 0.5 mL methanol. Both of them were collected, passed through a 0.22 μm Millipore filter, and injected onto a semi-preparative HPLC column using a flow rate of 5 mL/min and the gradient described above. The heart was homogenized using a Labgen 7 homogenizer, suspended in 1 mL methanol, and centrifuged for 5 min at 13,000 rpm. After removal of the supernatants, the pellets were washed with 0.5 mL of methanol. All the methanol solution was passed through a Sep-Pak C18 cartridge, and washed with 0.5 mL water and 0.5 mL methanol. Both of them were collected, passed through a 0.22 μm Millipore filter, and injected onto a semi-preparative HPLC column using a flow rate of 5 mL/min and the gradient described above.

2.17. Ex vivo autoradiography

Heart from a normal SD rat was dehydrated with 30% sucrose solution at 4 °C, sectioned (30 μm) with a cryostat and thaw-mounted onto Superfrost microscope slides (LEICA, CM1900). Frozen sections were fixed in acetone at room temperature for 30 min, and then stored at −20 °C. Frozen sections were removed from the freezer and air-dried at room temperature, then incubated in 100 μL saline, 20 μmol/L rotenone solution or 20 μmol/L [^{19}F]FP2OP solution at room temperature for 30 min, respectively. After removing the above solution, 100 μL [^{18}F]FP2OP solution (about 14.1 kBq) was added to the sections and incubated at room temperature for 30 min. After washing with water and 40% ethanol solution, the sections were dried and subjected to autoradiography for 10 min. Radioactive images were developed and quantified in Cyclone Phosphoimager system (Perkin-Elmer Inc., Boston, MA).

2.18. Cardiac PET/CT imaging

All the animal protocols were approved by the Institute's Animal Care and Use Committee. For PET study, a healthy Chinese mini-swine (weight 15 kg) was anesthetized with an intravenous of a mixture of ketamine (25 mg/kg) and diazepam (1.1 mg/kg). Anesthesia was supplemented as needed.

PET data were obtained using a PET/CT system (Biograph 64; Siemens Healthcare). The animal was placed in a prone position on the PET/CT bed, and a venous catheter was established for imaging agent injection. 85 MBq of [^{18}F]FP2OP in 2 mL 5% ethanol solution was injected intravenously. The PET/CT scan was performed at 5, 15, 30 and 60 min after the tracer injection, respectively. After CT low dose scan for attenuation correction (Tube voltage 120 kV, Tube Current 50 mAs with CareDose4D, Collimation 24 × 1.2 mm, Rotation time 0.5 s, Pitch 1.2, Slice 3 mm), PET imaging for myocardial uptake evaluation was acquired. List mode with ECG gating, the scan time was 8 min. The images were reconstructed with a conventional filtered-back projection method using a Butterworth-ramp filter with a cutoff frequency of 1.25 cm^{-1}. The matrix size was 2.0 × 2.0 mm with 128 × 128 pixels, and the slice thickness was 3.125 mm. The regions of interest (ROI) were placed on the myocardium, liver and lung. The standardized uptake value (SUV) was calculated as follow: SUV = [mean ROI count (cps/pixel) × body weight (kg)]/[injected dose (mCi) × calibration factor (cps/pixel)].

3. Results

3.1. Chemistry

The precursor OTs-P2OP was synthesized according to Figure 1 with good yield and characterized by ^{1}H NMR, ESI-MS and IR. The preparation procedure of nonradioactive [^{19}F]FP2OP is also shown in Figure 1. The structure of the desired nonradioactive compound was confirmed by ^{1}H NMR, ^{13}C NMR, ^{19}F NMR, ESI-MS, and IR analysis. The HPLC chromatogram shows that [^{19}F]FP2OP has a very good chemical purity (>98% at λ = 254 nm), with a retention time of 21.7 min (Fig. 2A). Based on these results mentioned above, this [^{19}F]FP2OP compound is considered to be an acceptable referenced standard for the radioactive compound [^{18}F]FP2OP.

3.2. Radiochemistry

Starting from [^{18}F]F$^-$ in a Kryptofix 2.2.2./K_2CO_3 solution, the total reaction time, including final HPLC purification, is about 100 min. The overall radiochemical yield, corrected for decay is 41 ± 5.3% (n = 7), the RCP of the purified [^{18}F]FP2OP, >98%. The [^{18}F]FP2OP is well separated from the precursor OTs-P2OP (with a retention time of 24.7 min, the HPLC profile was shown in Figure 2C). The specific activity of [^{18}F]FP2OP is estimated by radio-HPLC to be about 180 GBq/μmol,with a retention time of 22.1 min (Fig. 2B).

3.3. Partition coefficient (log *P*) of [^{18}F]FP2OP

The measured partition coefficient (log P) of [^{18}F]FP2OP is log P = 2.20 ± 0.00 (n = 3), suggesting that the compound was lipophilic.

3.4. Stability of [^{18}F]FP2OP

Figure 3A indicates that about 78.3% of the total ^{18}F was eluted at 21.5 min, while Figure 3C indicates that about 66.6% of the total ^{18}F was eluted at 20.5 min, suggesting that some decomposition of [^{18}F]FP2OP occurred during the 1 h incubation period in water or in

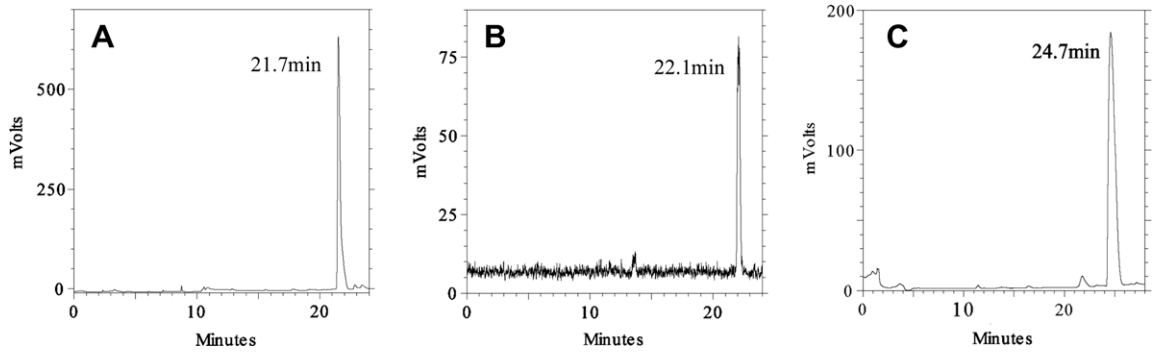

Figure 2. The HPLC chromatograms of [^{19}F]FP2OP (A) and OTs-P2OP (C) as well as the radiochromatogram of [^{18}F]FP2OP (B). The retention time of [^{19}F]FP2OP (21.7 min) and OTs-P2OP (24.7 min) were measured with a UV detector while the retention time of [^{18}F]FP2OP (22.1 min) was measured radiometrically.

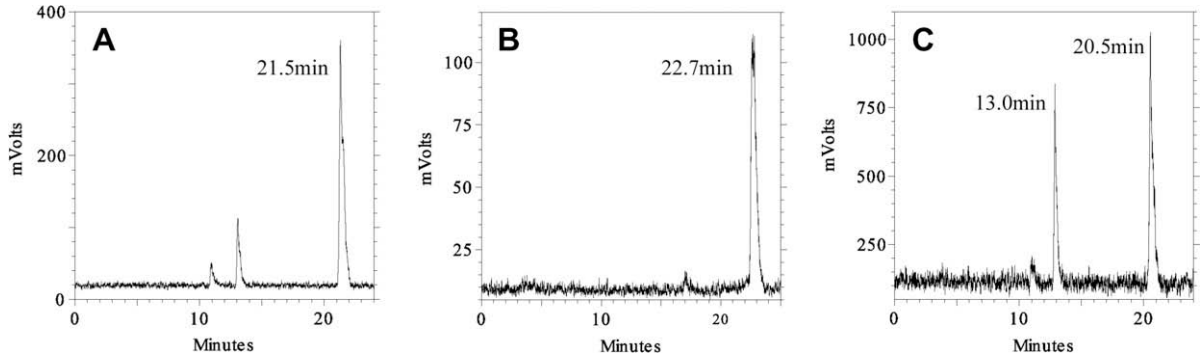

Figure 3. The radiochromatograms of [^{18}F]FP2OP after storage in water at room temperature for 1 h (A), in 80% ethanol solution at room temperature for 4 h (B), and after incubation in murine plasma at 37 °C for 1 h (C).

murine plasma. The stability of [^{18}F]FP2OP in 80% ethanol solution was also tested and the results showed that there have more than 95% of the total ^{18}F was eluted at 22.7 min (Fig. 3B), suggesting that it could be stable in 80% ethanol solution over 4 h. Accordingly, the HPLC purified [^{18}F]FP2OP was stocked in 80% ethanol solution and diluted with saline to 5% ethanol solution for use.

3.5. Paper electrophoresis

In paper electrophoresis, more than 98% [^{18}F]FP2OP did not show any movement, indicating neutrality of this compound.

3.6. Biodistribution of [^{18}F]FP2OP in mice

Biological distribution results in mice for [^{18}F]FP2OP and ^{99m}Tc-MIBI are shown in Table 1, as a percentage of the Injected Dose per Gram of organ (%ID/g ± SD).

As described in Table 1, [^{18}F]FP2OP has a significant heart uptake. The initial heart uptake is 41.90 ± 4.52% ID/g at 2 min post-injection (p.i.) time, which is much higher than that of ^{99m}Tc-MIBI (15.61 ± 1.50%ID/g at 2 min p.i.). Meanwhile, a low ^{18}F uptake is observed in most of the other tissues, especially in liver and kidney. The liver uptake of [^{18}F]FP2OP is 6.14 ± 0.48% ID/g at 2 min p.i., while for ^{99m}Tc-MIBI, 20.92 ± 5.14% ID/g at 2 min p.i. The ratios of heart/liver, heart/lung and heart/blood are 6.83, 9.49 and 35.74, respectively at 2 min after injection, thus making the material suitable to be a new myocardial perfusion imaging agent.

3.7. Metabolic stability

The metabolic stabilities of [^{18}F]FP2OP were determined in the heart, blood and urine of Kunming mice at 2, 30 and 60 min after injection. The HPLC analysis results of the fractions are shown in Figure 4. The heart radiochromatograms (Fig. 4A–C), indicates that

Table 1
The biodistribution of [^{18}F]FP2OP and ^{99m}Tc-MIBI in normal mice. Expressed as% injected dose per gram (% ID/g ± SD), n = 5

	[^{18}F]FP2OP				^{99m}Tc-MIBI	
	2 min	15 min	30 min	60 min	2 min	60 min
Heart	41.90 ± 4.52	33.54 ± 4.04	28.07 ± 2.11	24.80 ± 0.71	15.61 ± 1.50	15.62 ± 1.42
Liver	6.14 ± 0.48	5.92 ± 0.55	5.37 ± 0.53	4.80 ± 0.53	20.92 ± 5.14	13.74 ± 3.06
Spleen	2.60 ± 0.54	2.11 ± 0.12	2.48 ± 0.22	2.41 ± 0.22	5.17 ± 0.64	1.18 ± 0.25
Lung	4.42 ± 0.61	2.54 ± 0.51	2.98 ± 0.31	3.17 ± 0.14	6.93 ± 0.44	1.09 ± 0.10
Muscle	4.68 ± 0.85	9.24 ± 1.82	9.11 ± 3.25	9.74 ± 1.74	5.62 ± 0.779	5.53 ± 0.48
Bone	1.61 ± 0.26	2.10 ± 0.20	2.25 ± 0.30	3.70 ± 0.39	3.66 ± 0.74	1.54 ± 0.78
Kidney	18.43 ± 2.11	13.02 ± 0.82	11.59 ± 2.18	9.25 ± 1.55	37.78 ± 6.02	21.16 ± 2.84
Blood	1.17 ± 0.08	1.22 ± 0.29	1.98 ± 0.18	2.13 ± 0.14	2.16 ± 0.23	0.10 ± 0.01
Heart/liver	6.83	5.67	5.24	5.17	0.75	1.14
Heart/lung	9.49	13.22	9.41	7.82	2.25	14.35
Heart/blood	35.74	27.53	14.2	11.62	7.24	154.7

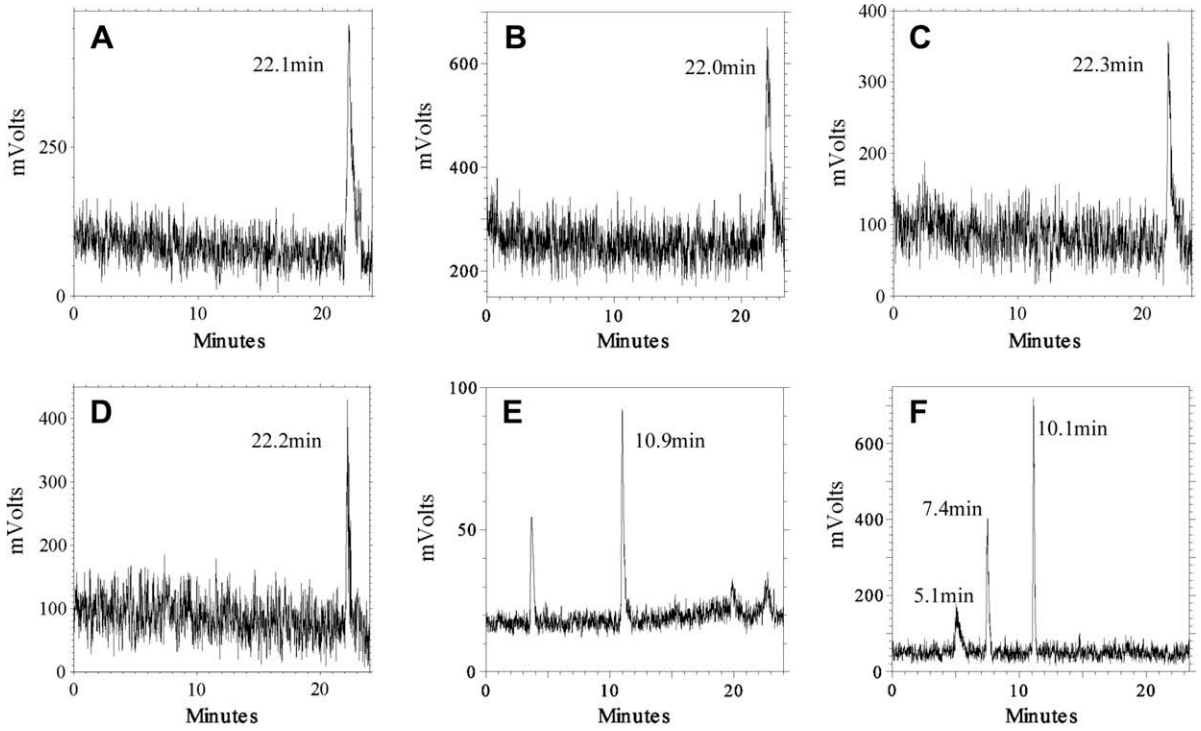

Figure 4. The HPLC profiles of soluble fractions of [^{18}F]FP2OP. Heart was collected at 2 min (A), 30 min (B) and 60 min (C) after injection; blood was collected at 2 min (D) and 60 min (E) after injection; and urine (F) was collected at 30 min after injection into a normal Kunming mouse.

more than 95% of the total ^{18}F was eluted at 22 min, suggesting that [^{18}F]FP2OP could be stable in the myocardium over 60 min after injection. At 2 min after injection, [^{18}F]FP2OP was stable in blood (Fig. 4D). While at 60 min after injection, the peak at 22.0 min has almost disappeared and two new peaks have appeared at 3.8 min and 10.9 min, suggesting that the compound undergoes considerable degradation in blood (Fig. 4E). Similarly, the urine radio chromatogram Figure 4F suggests that no intact [^{18}F]FP2OP was excreted in the urine and no defluorination of the [^{18}F]FP2OP appears to have occurred since increasing bone uptake was not observed (Table 1).

3.8. Ex vivo autoradiography

Ex vivo autoradiography studies were performed on heart frozen sections from a normal SD rat (Fig. 5). The autoradiogram shows that [^{18}F]FP2OP had high uptake in myocardium (Fig. 5B), and it could be blocked by both of pre-incubated with rotenone (Fig. 5C) and [^{19}F]FP2OP (Fig. 5D). The net intensity was calculated, the ratios of control to rotenone inhibited section and control to [^{19}F]FP2OP inhibited section were 4.0 and 2.6, respectively. The results of autoradiography suggesting that [^{19}F]FP2OP has the same binding site and comparable affinity with rotenone (a known MC-I inhibitor with high affinity). Based on autoradiography results, we believe that both of [^{19}F]FP2OP and [^{18}F]FP2OP compounds are potent inhibitors of MC-I.

3.9. Cardiac PET/CT imaging

The PET/CT studies of [^{18}F]FP2OP were performed in a healthy Chinese mini-swine. The representative PET images were displayed in Figure 6. High heart activity accumulation was observed. The SUVs of heart were 10.15 (5 min p.i.), 9.39 (15 min p.i.), 8.42 (30 min p.i.) and 5.83 (60 min p.i.). The clearance tendency was well agreed with that of biodistribution studies in mice. The outline of myocardium was clear and the uptakes in background organs (liver and lung) were very low at all time points. The SUVs of liver were 2.85, 2.69, 2.14 and 1.82 at 5, 15, 30 and 60 min p.i., respectively. The SUVs of lung were 0.69, 0.71, 0.64 and 0.39 at 5, 15, 30 and 60 min p.i., respectively. The clearance rate of activity from these organs have no significant difference, while in mice biodistribution studies the activity cleared from heart much faster than that of liver and lung. The heart/liver and heart/lung ratios were calculated as 3.56 and 14.71 (5 min p.i.), 3.49 and 13.23

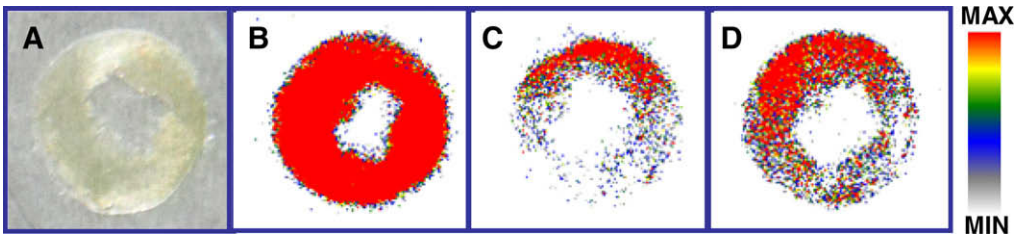

Figure 5. The autoradiograms of heart sections from a normal SD rat. The sections were incubated with 100 μL [^{18}F]FP2OP solution (about 14.1 kBq) for 30 min at room temperature pre-treated with 100 μL saline (B), 20 μmol/L rotenone (C) or 20 μmol/L [^{19}F]FP2OP (D), respectively. A is the photo of a heart section before subjected to autoradiography.

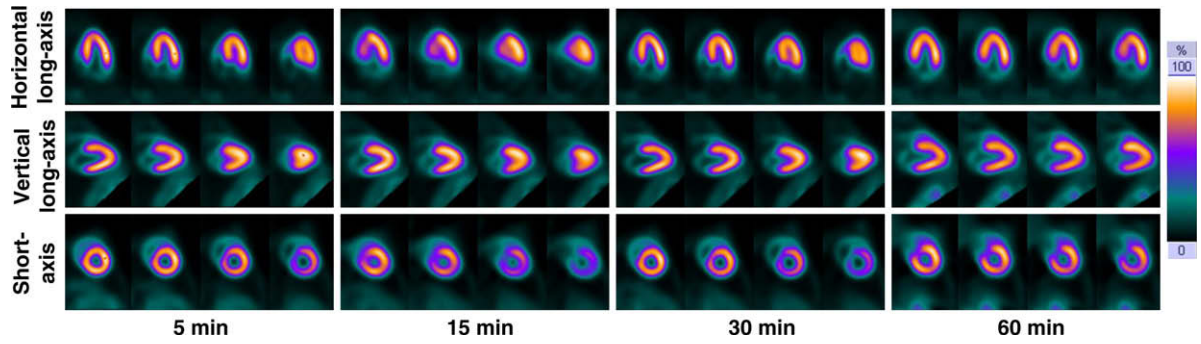

Figure 6. Cardiac PET images of a healthy Chinese mini-swine with 85 MBq [^{18}F]FP2OP in 5% ethanol solution. The images were collected at 5, 15, 30, 60 min after injection, respectively.

(15 min p.i.), 3.93 and 13.16 (30 min p.i.), 3.20 and 14.95 (60 min p.i.), respectively.

4. Discussion

In the early 1990s, several novel ^{99m}Tc-labeled perfusion tracers (^{99m}Tc-MIBI, ^{99m}Tc-tetrofosmin and ^{99m}TcN-NOEt) had been developed for SPECT myocardial perfusion imaging. Among those agents, ^{99m}Tc-MIBI has been accepted worldwide for evaluation of CAD with SPECT imaging. Thence forwards, several new MIBI complexes (^{99m}TcN-MIBI[19] and ^{99m}Tc(CO)$_3$(MIBI)$_3$[20]) with different ^{99m}Tc core have been reported for myocardial perfusion imaging. All of them have improved biodistribution properties in the mouse when compared with ^{99m}Tc-MIBI.

Very recently, there is increasing interest in and actual use of PET for myocardial perfusion imaging[21] and several new ^{18}F-labeled tracers have been reported as mitochondrial complex I (MC-I) inhibitors and evaluated for this purpose. In 2004, Marshall et al. reported an ^{18}F-labeled rotenone analogue (^{18}F-FDHR) and it was evaluated in the isolated rabbit heart as a new myocardial flow tracer.[8] Unfortunately, there are no further in vivo data of it being reported till now. Studies by Yu et al.[6,9,22] indicate that BMS-747158-02 is a novel ^{18}F-labeled pyridazinone derivative designed for cardiac imaging, and it represents a new class of PET myocardial perfusion imaging agent. Cardiac imaging with this agent shows clear myocardium and identification of the perfusion deficit area in rats, rabbits, pigs, nonhuman primates, and human subjects.

In this study, we report the synthesis of a new ^{18}F-labeled pyridaben analogue: [^{18}F]FP2OP as a MPI agent. The physicochemical properties, stabilities and biodistribution in mice of this compound were evaluated. Compared with other MPI agents, [^{18}F]FP2OP had a much higher heart uptake. Even at 60 min after injection, the heart uptake was 24.80 ± 0.71% ID/g, which was still higher than that of ^{99m}Tc-MIBI (15.62 ± 1.42% ID/g at 60 min after injection) and ^{18}F-BMS-747158-02 (9.5% ± 0.5% ID/g at 60 min after injection).[23] Furthermore, the heart/liver ratios of [^{18}F]FP2OP were 6.83 and 5.17 at 2 min and 60 min, respectively after injection, which were comparable with the other reported ^{18}F-labeled mitochondrial complex I inhibitors.[6,9,22] The results of the biodistribution in vivo indicated that the [^{18}F]FP2OP had rapid and high uptake in the heart and low background uptake in the blood, liver and lung of the mouse. Compared with ^{99m}Tc-MIBI, the [^{18}F]FP2OP had much higher heart/liver ratios at all time points after injection and higher heart/lung and heart/blood ratios at earlier time point (2 min after injection) than that of ^{99m}Tc-MIBI (Table 1).

The results of autoradiography showed that this new compound has the same binding site and comparable affinity with rotenone, a well know MC-I inhibitor, and it could be developed as a potent inhibitor of MC-I for myocardial perfusion imaging. The high quality images of myocardium were obtained in PET/CT study of healthy Chinese mini-swine. The high initial heart uptake and low background uptake at earlier time point make it possible for performing imaging at earlier time with minimal injection dose. It is also worth mentioning that the fast myocardium clearance of [^{18}F]FP2OP could lower the irradiation dose and make it a good choice for stress and rest imaging in one-day protocol. All of the properties of [^{18}F]FP2OP reported here make it could be superior to the other MPI agents.

5. Conclusion

A novel ^{18}F-labeled compound [^{18}F]FP2OP has been successfully prepared in high yield and high radiochemical purity (>98%). Based on the results of the experiments reported here comes a conclusion that [^{18}F]FP2OP is a lipophilic and neutral complex. The biodistribution studies in mice shows that this compound has a significant high heart uptake, and good heart/liver, heart/lung, heart/blood ratios. Cardiac PET imaging in a healthy Chinese mini-swine shows clear outline of myocardium at all time points, suggesting the potential usefulness of this compound as a myocardial perfusion imaging agent.

Acknowledgments

This work was supported by the National Natural Science Foundation of China (20871020) and Beijing Natural Science Foundation (2092018). The authors wish to acknowledge the Beijing SHIHONG Pharmaceutical Co, Ltd for the donation of MIBI Kits. Dr. Yuanqun Jiang is acknowledged for her useful comments and suggestions on the language of our manuscript.

Supplementary data

Supplementary data associated with this article can be found, in the online version, at doi:10.1016/j.bmc.2009.12.022.

References and notes

1. Russell, R. R.; Zaret, B. L. *Curr. Probl. Cardiol.* **2006**, *31*, 557.
2. Madar, I.; Ravert, H. T.; Du, Y.; Hilton, J.; Volokh, L.; Dannals, R. F.; Frost, J. J.; Hare, J. M. *J. Nucl. Med.* **2006**, *47*, 1359.
3. Bateman, T. M. *Am. J. Cardiol.* **2004**, *94*, 19.
4. Kronauge, J. F.; Chiu, M. L.; Cone, J. S.; Davison, A.; Holman, B. L.; Jones, A. G.; Piwnica-Worms, D. *Int. J. Radiat. Appl. Instrument. B, Nucl. Med. Biol.* **1992,** *19*, 141.
5. Cheng, Z.; Subbarayan, M.; Chen, X.; Gambhir, S. S. *J. Label. Compd. Radiopharm.* **2005**, *48*, 131.
6. Yu, M.; Guaraldi, M. T.; Mistry, M.; Kagan, M.; McDonald, J. L.; Drew, K.; Radeke, H.; Azure, M.; Purohit, A.; Casebier, D. S.; Robinson, S. P. *J. Nucl. Cardiol.* **2007**, *14*, 789.

7. Marshall, R. C.; Powers-Risius, P.; Reutter, B. W.; Taylor, S. E.; VanBrocklin, H. F.; Huesman, R. H.; Budinger, T. F. *J. Nucl. Med.* **2001**, *42*, 272.
8. Marshall, R. C.; Powers-Risius, P.; Reutter, B. W.; O'Neil, J. P.; La Belle, M.; Huesman, R. H.; VanBrocklin, H. F. *J. Nucl. Med.* **2004**, *45*, 1950.
9. Yu, M.; Guaraldi, M.; Kagan, M.; Mistry, M.; McDonald, J.; Bozek, J.; Yalamanchili, P.; Hayes, M.; Azure, M.; Purohit, A.; Radeke, H.; Casebier, D. S.; Robinson, S. P. *Eur. J. Nucl. Med. Mol. Imaging* **2009**, *36*, 63.
10. Yang, W.; Mou, T.; Peng, C.; Wu, Z.; Zhang, X.; Li, F.; Ma, Y. *Bioorg. Med. Chem.* **2009**, *17*, 7510.
11. Zhang, X.; Cai, W.; Cao, F.; Schreibmann, E.; Wu, Y.; Wu, J. C.; Xing, L.; Chen, X. *J. Nucl. Med.* **2006**, *47*, 492.
12. Feng, Y.; Yang, X.; Rong, W.; Niu, R. *Hebei Chem. Eng. Ind.* **2000**, *3*, 27.
13. Bender, J. L.; Shen, Q.-D.; Fraser, C. L. *Tetrahedron* **2004**, *60*, 7277.
14. Casebier, D. S.; Robinson, S. P.; Purohit, A.; Radeke, H. S.; Azure, M. T.; Dischino, D. D. U.S. Patent, United State Patent Application Publication, Pub. No.: US 2005/0191238 A1 2005.
15. Zhang, X.; Zhou, P.; Liu, J.; Huang, Y.; Lin, Y.; Chen, Y.; Gu, T.; Yang, W.; Wang, X. *Appl. Radiat. Isot.* **2007**, *65*, 287.
16. Mou, T.; Yang, W.; Peng, C.; Zhang, X.; Ma, Y. *Appl. Radiat. Isot.* **2009**, *67*, 2013.
17. Cai, W.; Zhang, X.; Wu, Y.; Chen, X. *J. Nucl. Med.* **2006**, *47*, 1172.
18. Zhang, X.; Xiong, Z.; Wu, Y.; Cai, W.; Tseng, J. R.; Gambhir, S. S.; Chen, X. *J. Nucl. Med.* **2006**, *47*, 113.
19. Zhang, X. Z.; Wang, X. B.; Jia, F.; Tang, Z. G.; Zhang, J. B.; Liu, B. L.; Wang, X. Y. *J. Label. Compd. Radiopharm.* **2002**, *45*, 1029.
20. Hao, G.; Zang, J.; Zhu, L.; Guo, Y.; Liu, B. *J. Label. Compd. Radiopharm.* **2004**, *47*, 513.
21. Glover, D. K.; Gropler, R. J. *J. Nucl. Cardiol.* **2007**, *14*, 765.
22. Yu, M.; Guaraldi, M. T.; Bozek, J.; Kagan, M.; Azure, M.; Radeke, H.; Cdebaca, M.; Robinson, S. P. *J. Nucl. Cardiol.* **2009**, *16*, 763.
23. Yalamanchili, P.; Wexler, E.; Hayes, M.; Yu, M.; Bozek, J.; Kagan, M.; Radeke, H.; Azure, M.; Purohit, A.; Casebier, D.; Robinson, S. *J. Nucl. Cardiol.* **2007**, *14*, 782.